# Soft Robot Actuation Strategies for Locomotion in Granular Substrates

Daniel Ortiz[1], Nick Gravish[1], and Michael T. Tolley[1]

***Abstract*—Soft bodied organisms such as annelids may exploit body compliance using their hydrostatic skeletons and muscles to burrow in granular substrates. In this work, we investigate the design of soft digging robots inspired by the bristled worm, (polychaetas). The behavior of soft structures in dry granular environments is complex and still not well understood. We describe the design and fabrication of a soft robot capable of locomotion in granular substrates and investigate actuation strategies for drag reduction inspired by the bristled worms biomechanical behaviors. The drag reduction experiments focus on an actuated soft leading segment. We implemented and studied two methods of actuation for the leading segment: periodic radial expansion and bi-directional bending, both of which we find to have an impact on locomotion in granular substrates. Soft robots performing periodic radial expansion of the leading segments experienced the least overall drag force, while those with unactuated tips experienced the largest drag force, emphasizing the importance of controlling the tip stiffness to enable effective subsurface movement. Based on these results, we designed and tested a tethered, three-segment soft robot capable of digging through dry granular media.**

***Index Terms*—Soft Robot Applications, Soft Robot Materials and Design, Modeling, Control, and Learning for Soft Robots, Field Robots**

## I. Introduction

GRANULAR substrates (GS) are collections of solid particles. Examples of natural GS range from rubble and sand to a variety of soils. These materials can behave as a fluid, solid, and gas, depending on the loading conditions. When an external perturbation is applied, these materials can transition between these states and generate complex reaction forces. Rigid robotic systems typically perform well on hard, flat surfaces, yet movement across granular substrates can be challenging and may require special wheels or continuous tracks. Furthermore, movement within these substrates, as required for applications such as construction, environmental monitoring, and surveillance, is a challenge for conventional robotic systems. We propose to address this challenge with a soft robot inspired by the bristle worm (polychaetas).

The study of granular substrates and flowing particle interaction is comprehensive [1], [2], [3], [4], [5], [6], [7], [8], [9], [10], [11]; however, there are limited studies for how compliant systems interact in these dynamic materials [12], [13]. Scientists and engineers have turned to animals and the principles surrounding their locomotion to solve many problems of robot mobility in a wide range of environments [14], [15], [16], [17], [18]. In the context of locomotion on and within granular substrates, this bioinspired approach has proven successful in producing novel robot designs, gaits, and control methods. For example, the sidewinder rattlesnake (*Cortalus cerastes*) inspired a robot capable of traversing sloped GS [19]; the razor clam (*E. directus*) inspired a system capable of burrowing by fluidization [20]; and the sandfish lizard (*S. Scincus*) inspired another system for swimming through GS [21]. Other work has studied strategies for legged locomotion and for walking on deformable substrates inspired by a variety of lizards and crabs [22], [23].

Although the previous examples have solved the problem of moving in and on GS with rigid robots, most animals are not completely rigid and are instead composed of tissues that exhibit a range of stiffnesses (e.g. skin, muscles, fat, cartilage, bones, and tendons). The resulting compliance of their bodies allows animals to conform to complex shapes in various terrains, and to absorb impacts when in motion. Recently, scientists have incorporated compliance in a novel soft robot design that is capable of tip extension and granular fluidization to maneuver in granular materials [12]. Fluidization of granular materials is a technique that is used by bivalves and some species of crabs to loosen granular material in their paths and reduce the friction between the particles.

Incorporating soft materials into robotic systems provides many advantages for maneuvering on and in GS, including enhanced durability of the system, the ability to conform the robots body to surroundings, and robust actuation in these unstructured environments [15], [24], [25], [26]. For this study, we take inspiration from polychaetas, a class of marine annelids that live and burrow in granular environments Polychaetas exhibit a range of behaviors during locomotion including 1) bi-directional bending (side-to-side head movement) to remove material from its path; 2) radial expansion to anchor their position while elongating forward, effectively expanding the cavity through crack propagation; 3) rapid eversion of a proboscis to quickly expand the burrowing cavity [27], [28], [29]. For example, Polychaetas (*Nereis diversicolor*) are capable of burrowing in underwater granular substrates to depths reaching a maximum of approximately 29 cm. The burrowing depth depends on food supply and predation risk [30]. Understanding these mechanisms may provide insight into locomotion in GS and aid in understanding the forces being exerted on soft deformable bodies.

Of the strategies described above, peristaltic motion and

Manuscript received: 10, 15, 2018; Revised 2, 11, 2019; Accepted 3, 15, 2019.

This paper was recommended for publication by Editor Kyu-Jin Cho upon evaluation of the Associate Editor and Reviewers' comments. This work was supported by the National Science Foundation (NSF award #1837662)

[1]All authors are with School of Mechanical & Aerospace Engineering Department, University of California, San Diego tolley@ucsd.net

Digital Object Identifier (DOI): see top of this page.

This article has been accepted for publication in a future issue of this journal, but has not been fully edited. Content may change prior to final publication. Citation information: DOI 10.1109/LRA.2019.2911844, IEEE Robotics and Automation Letters



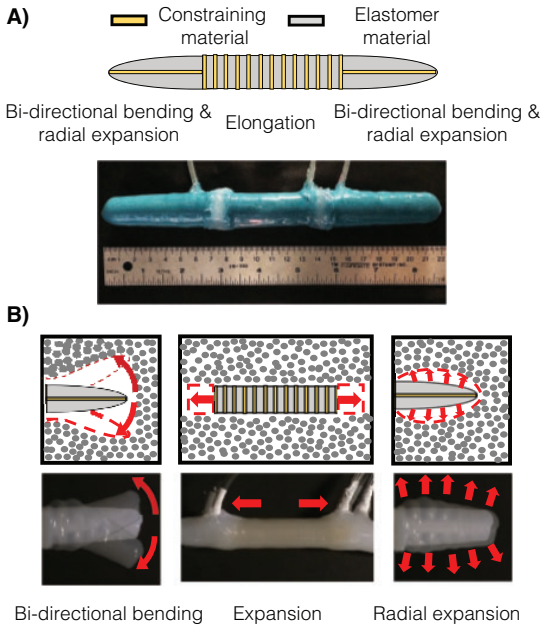


Fig. 1. Bioinspired actuation strategies for a soft robot capable of digging in granular media. (A) Schematic and image of the soft robotic system dyed green for visualization in clear granular material. (B) Schematic and image of biomechanical digging behaviors (bi-directional bending and radial expansion, and elongation).

bi-directional bending are the most amenable to replication in a soft robotic system (Fig. 1B). Peristaltic motion is generated by volumetric expansion and contraction of radial and longitudinal muscles in retrograde waves. This wave of muscular contractions allows annelids to apply normal force on the burrow walls, and thus anchor their position in unstructured terrain while elongating forward [27]. Previous work has used soft robotic systems inspired by earthworms to model and replicate peristaltic motion [31], [32]. Although numerous attempts have been made to replicate this biomechanical behavior through various techniques [31], [32], [33], [34], [35], [36], no attempts have been made in demonstrating and examining the drag forces in unstructured dry granular environments. Much of the previous work has examined the biomechanical behaviors in structured environments such as piping, vents, and along relatively smooth surfaces.

Bi-directional bending (side-to-side head movement) is observed when Polychaetas (*Nereis virens*) are burrowing in stiffer materials, to relieve compressive forces on them [27]. No work has previously implemented this in a soft robotic system for digging.

This paper presents experimental validation that Polychaeta inspired behaviors and compliant materials can be implemented in robotic applications for drag reduction and locomotion in dry granular environments. This study has the potential to help with various applications such as construction, pipe inspection, exploration of hazardous environments e.g. avalanches and earthquakes, and subsurface exploration on other planets. The remainder of this paper discusses the experimental design decisions, the fabrication of the soft robotic system, and experimental methods in Section II. Section III describes the results, and Section IV discusses the findings.

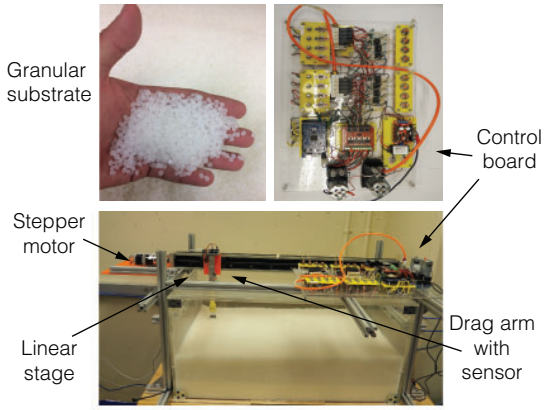


Fig. 2. Experimental enclosure used for constant velocity experiments and control system for actuating the soft-robot. Images of the experimental enclosure (bottom), the polypropylene pellets (top-left), pneumatic control system (top-right).

We provide concluding remarks in Section V.

## II. Methods

### A. Experimental Design

To examine the drag exerted on the deformable robot in GS, we ran several experiments focused on the tip of the robot. For these experiments, we designed and fabricated a custom acrylic dry granular enclosure (Fig. 2). In separate experiments, we prescribed either a constant velocity or a constant force to an arm dragged through the GS with a soft robotic leading segment attached. We then measured the corresponding force onor velocity ofthis soft robotic segment (respectively). We chose to compare four soft robot leading segment designs: 1) one capable of periodic radial expansion, 2) one capable of bi-directional bending, 3) an unactuated soft intruder, and 4) an unactuated rigid intruder (with a thin silicone skin to keep the friction coefficient constant). To determine the drag effects due to the experimental setup, we also performed baseline experiments with no intruders attached.

As a final experiment, we submerged an entire three-segment, tethered soft robot worm in the dry granular media and tracked its position during unassisted locomotion. We supported the pneumatic tethers above the tank to prevent any kinking or dragging and allowed them to follow the robot in the direction of motion without tension by increasing the slack. To compare this last experiment against an ideal case of unassisted locomotion, we also ran an experiment in which the soft robot crawled through a smooth acrylic tube with no granular media present.

### B. Robot Design, Fabrication, and Actuation

The soft robotic system consisted of three silicone pneumatic actuators in series. We selected three actuators because it is the minimum number required to generate peristaltic motion, although more segments could be added. Soft actuators can be mechanically programmed to expand, twist, bend, and elongate

This article has been accepted for publication in a future issue of this journal, but has not been fully edited. Content may change prior to final publication. Citation information: DOI 10.1109/LRA.2019.2911844, IEEE Robotics and Automation Letters



by varying the orientation of the constraining material and the geometry [37]. To generate the desired bending motion for our soft robotic system, we designed a series of pneumatic networks or Pneu-nets which utilized a thinner geometry between the channels [38]. To generate bending in two directions we included a strain limiting layer between two sets of Pneu-nets. To constrain the radial expansion of elongation segments, we wrapped polyaramid thread around the circumference of a hollow elastomeric tube (Fig. 1A).

We chose a platinum cured silicone elastomer (Dragon Skin 10, Smooth-On) for the actuators because of its low stiffness (Shore value of 10A). This silicone elastomer has amorphous characteristics which allow it to elongate up to a maximum of 663% allowing the robotic actuators to be inflated at relatively low pressures with a minimum actuation pressure of 55 kPa for our design (Fig.1).

We delivered pressurized air separately to each of these segments through silicone tubes. For a robot capable of both bi-directional bending at the leading segment and peristaltic motion a minimum of four pneumatic lines are needed: Two pneumatic lines for the leading intruder, and one for each of the two other segments.

We connected the tubing to the soft robot perpendicular to the plane of motion for simplicity and to help us visually track its movement with red markers when it was submerged in the GS. The orientation of the pneumatic lines produced additional anchoring in the granular material as a byproduct of the experiments, thus these experiments represent a worst-case scenario for future untethered systems.

To fabricate the soft robot, we first designed the negative of each actuator in computer-aided design (CAD) software. We then 3D printed a mold of the negative and cast actuator halves in these molds from the two-part silicone elastomer with a 1:1 mixture ratio. After curing the two halves, we bonded them to a central constraining (flexible but inextensible) layer with a silicone adhesive, creating two independent chambers for the leading actuator. To make an elongating motion in the middle actuator, we constrained radial expansion by manually wrapped polyaramid thread around the radius.

After assembling the segments, we manually coated them with two layers of silicone to seal the constraining materials. All the intruders used for the actuated leading segments were conically shaped, approximately 7 cm in length with a base diameter of 2.5 cm, tapering to a tip diameter of 1.8 cm. To assemble the three-segment robotic system, we bonded an alternating pattern of expanding/bending segments followed by elongating segments, independently sealed and separated by nonwoven polyester/cellulose cloth (Fig. 1A). After bonding, we inserted pneumatic lines to each segment and sealed them using silicone adhesive.

To fabricate the rigid intruder for the drag experiments, we 3D printed a positive of the part out of polylactic acid (PLA) and added two layers of the same silicone material to keep the surface friction constant. To isolate the leading segment for the constant force and velocity experiments, we attached a silicone plate with a thickness approximately the same as the largest diameter of the robot and press-fit the intruder into a rigid bracket (Fig. 3).

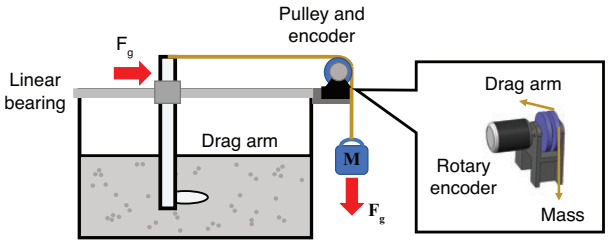


Fig. 3. Diagram of constant force experimental setup (left) and model of the pulley and encoder (right) used to measure velocity of the drag arm using a rotary encoder to collect position data.

To control the actuation of the soft components for all the experiments we used an open-source fluidic control board [39] (Fig. 2). For the drag experiments, the control board opened and closed valves connecting a source of pressurized air to the segments being actuated. We experimentally determined that an open time of 2.3 s corresponded to the maximum actuation amplitude without causing failure. We also used this timing for the initial experiments with the unassisted tethered three-segment soft robot for a complete peristaltic cycle of approximately 7 s. Furthermore, biological annelids have a similar stride period of 2.5 s [40]. We found that a constant source pressure of approximately 96 kPa achieved 80% of the bending amplitude, and that the maximum bending occurred near failure at 110 kPa.

After running tethered experiments with the entire soft robot in both the acrylic tube and the dry granular media, we adapted our control strategy to increase the velocity of the robot by decoupling the actuation timing from amplitude. To achieve this, we decreased the open time of valves connecting the pressure source to the radially expanding segments using pulse-width modulation (PWM), and increased the open time (duty cycle) of the extending middle segment, to increase the relative extension of the robot during each cycle without causing the expanding segment to fail.

### C. Dry Granular Substrate Enclosure

We performed all the experiments for this work in an acrylic enclosure filled with smooth dry plastic polypropylene pellets (Fig. 2). These particles where chosen because of their heterogeneous ellipsoidal shape, and most importantly because this material has a low volume fraction of 0.5, similar to a sand-silt mixture [41]. We chose these particles instead of sand because of their scale in comparison to the soft robot. The volume fraction for the polypropylene pellets was calculated as $\phi = \frac{V_p}{V}$ where $\phi$ denotes the volume fraction, $V_p$ the volume of the particles, and $V$ the total volume. The volume fraction plays a very important role in the dynamics of GS in response to stress [42]. We chose a depth of 5 cm for all the assisted experiments because it was the lowest depth at which movement was visible at the surface.

Finally, for visualization of the soft robotic peristaltic cycle, we used spherical hydrogel beads and water to create a transparent effect, as seen in the supplementary video. Note that this submerged setup was used for visualization purposes only, not for collecting experimental data.

This article has been accepted for publication in a future issue of this journal, but has not been fully edited. Content may change prior to final publication. Citation information: DOI 10.1109/LRA.2019.2911844, IEEE Robotics and Automation Letters



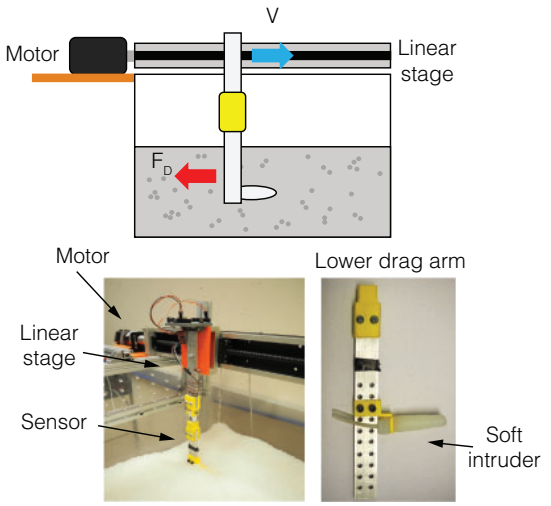


Fig. 4. Diagram (top) and images (bottom) of constant velocity experimental setup. This experiment was used to measure the drag forces experienced by various digging soft-robot segment configurations.

### D. Constant Force Single-Segment Experiments

To measure the steady-state velocity of soft robotic segments in GS, we attached them to a linear slide and applied a constant force to the segment with a weight (Fig. 3). To measure the displacement, we used an incremental rotary encoder (Signswise) with 600 pulses per revolution (PPR) resolution attached to a pulley that turned as the slide moved.

Initially, we determined the range of applied forces to use with some basic experiments: We incrementally loaded the system until we reached the minimal mass required to overcome the resistive force of the material and initiate movement for each of the four configurations (no actuation both rigid and soft, radial expansion, and bi-directional bending). Based on these tests, we chose the constant forces for this experiment to be 4.5 N, 6 N, 7.5 N, and 9 N. We also chose to use an experiment length of approximately 300 mm located near the center of the enclosure to minimize boundary effects.

In a first set of tests, a constant force was applied until the segment and drag arm traveled 300 mm or fell below a threshold velocity of 0.01 mm/s. These experiments all started with the soft intruder held at rest until the actuation was initiated at which point it was released. We ran this experiment three times for each method of actuation for each of the four constant forces. The particle bed was raked and mixed before each new trial to ensure the removal of any compactions in the material due to settling.

### E. Constant Velocity Single-Segment Experiments

To measure the drag force during a constant displacement, we used a linear stage with an attached aluminum with a load cell capable of measuring up to 98 N of force with a 0.01 N resolution (TAL 220, HT Sensor Technology Co.) (Fig. 4). The linear stage was driven using a 15:1 geared stepper motor (NEMA 23, Dongyang Dongzhueng Motor Co.) capable of generating enough torque to overcome the resistive force of the granular material. We ran the experiment at constant

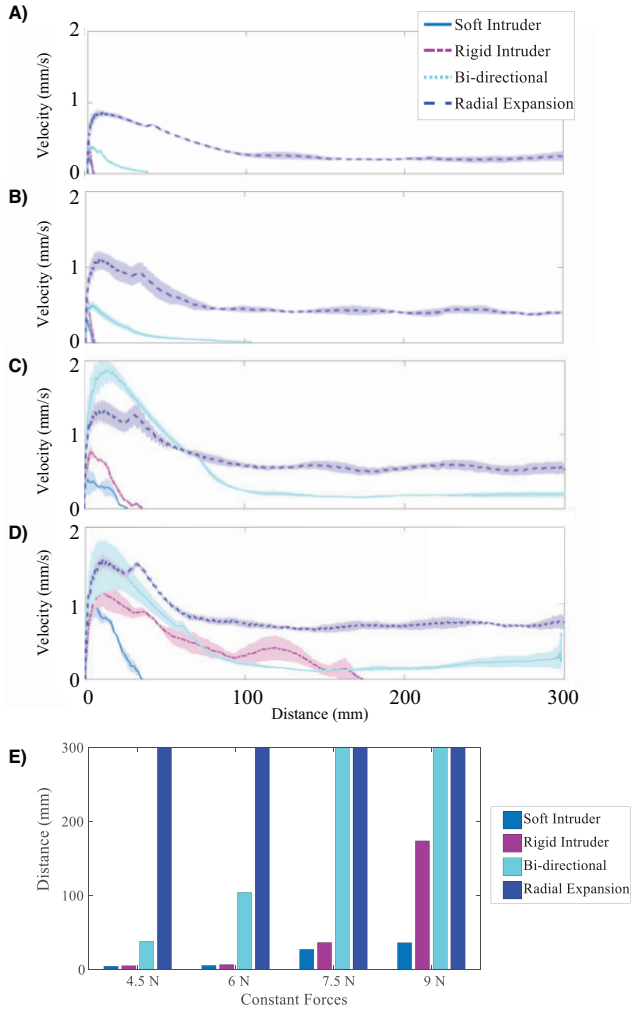


Fig. 5. Results of constant force experiments where position data was collected using a rotary encoder. Shaded regions represent the standard error for three trials. (A)-(D) Raw data for four applied forces A) 4.5 N, (B) 6 N, (C) 7.5 N, and (D) 9 N. E) Bar graph summarizing distances traveled for all four constant force cases for the different soft-robot segment configurations.

velocities of 0.5 mm/s, 1 mm/s, and 2 mm/s. We chose these speeds based on the speeds measured during the constant force experiments. The embedded load cell measured the deflection of the arm to calculate the resistive force impeding motion. We measured the drag force for the same four configurations of the leading segment: 1) bi-directional bending; 2) periodic radial expansion; 3) soft, unactuated; 4) rigid, unactuated.

The constant velocity experiments started with the leading intruder being actuated immediately followed by the linear stage being driven by the stepper motor. We performed this experimental sequence to ensure the soft intruder would not start off being forced to the side of least resistance and influence the measured deflection of the aluminum arm. We then continued the experiment over a 300 mm distance, after which we shut off the robot segment actuation and stepper motor. The experiment was then allowed to settle until the force measurement was near zero. The experiments were performed a total of three times for each method of actuation for all three constant velocities. The granular bed was raked and thoroughly mixed prior to each of the trials. Lastly, to

This article has been accepted for publication in a future issue of this journal, but has not been fully edited. Content may change prior to final publication. Citation information: DOI 10.1109/LRA.2019.2911844, IEEE Robotics and Automation Letters



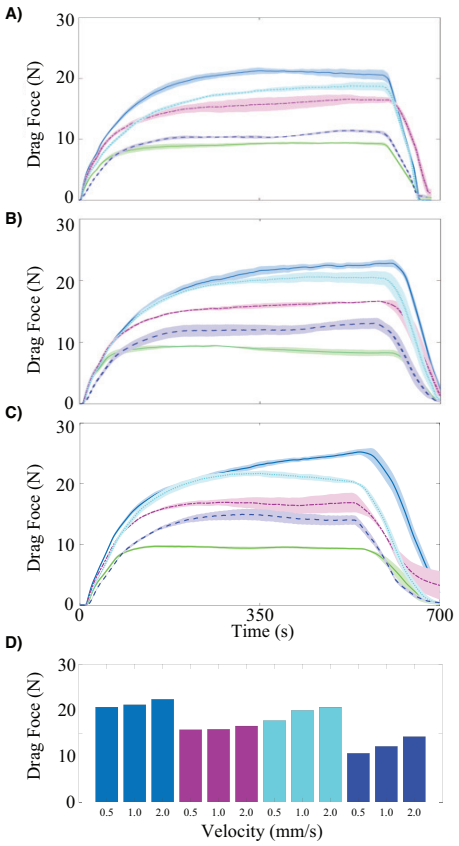


Fig. 6. Results of constant velocity experiments where displacement of the aluminum drag arm was measured and the resistive force was determined. (A)-(C) Raw data of the constant velocity experiments: (A) 0.5 mm/s, (B) 1 mm/s, and (C) 2 mm/s. Shaded regions represent standard error. Bar graph of the average drag force for each constant velocity for all four actuation configurations (D).

measure the drag force that the system was experiencing without intruders attached, we ran the same tests and measured drag on the aluminum arm alone.

### *F. Tethered Three-Segment Digging*

To verify the tethered soft robot could maneuver without assistance and to examine the best performing behavior to reduce the drag force, we ran an experiment using peristaltic actuation to generate self-propelled motion. For these experiments, we submerged the soft robot up to red markers we placed on the pneumatic lines in the center of the tank away from the walls to minimize any effects due to the boundaries. We attached a string to the soft robot and the other end was spooled around a reel with a mounted encoder. As the soft robot moved forward, the unspooling string rotated the pulley, providing the displacement of the robot. We ran this experiment until the velocity of the robot decreased below a threshold of 0.01 mm/s. As before, we raked the particles prior to each experiment.

As a point of comparison, we also tested the system in an acrylic pipe with a 35 mm inner diameter to get a comparison of the ideal performance scenario in a structured environment. We also modified the PWM duty cycle of the gate sequence to increase the extension of the middle segment of the robot and in turn increase the digging velocity in dry granular media. We ran a total of six trials for the three-segment tethered soft robot experiments, two in dry granular media with the same frequency used for the actuated tip experiments, two in dry granular media with modified PWM and decreased gait frequency, and we visually recorded two experiments in a smooth acrylic pipe with no dry granular media present. To help with visualization of the peristaltic cycle that we used for the tethered experiments we recorded the soft robot submerged in spherical hydrogel beads with water to get a transparent media.

## III. Results

### *A. Constant Force Single-Segment Experiments*

The results of the constant force experiments can be seen in Fig. 5. The periodic radial expansion achieved the highest steady-state velocity for all the cases. The radial expansion configuration was also able to move the entire 300 mm distance without getting stuck, for all cases of constant force. The soft robot segment configuration that was able to achieve the second highest steady-state velocity for all cases of constant force was bi-directional bending. Both robot segments with no actuation (rigid and soft) got stuck in the granular material or fell below the threshold of 0.01 mm/s for every level of applied force. Of the unactuated robot segments, the soft unactuated segment moved the least (Fig. 5). We also observed two peaks in the velocity average of three trails.

### *B. Constant Velocity Single-Segment Experiments*

The results of the constant velocity experiments are summarized in Fig. 6D. The robot segment configuration of periodic radial expansion experienced the lowest drag force for all three cases of constant velocity (0.5 mm/s, 1 mm/s, and 2 mm/s, Fig. 6A-C). The rigid intruder experienced the second lowest drag force, and the intruder that experienced the most drag force was the soft unactuated intruder. The bi-directional bending configuration experienced slightly more drag force than the rigid robot segment configuration. The baseline for the aluminum arm with no attachments was consistent across all velocities tested, and less than the drag force measured for all the actuation methods.

### *C. Tethered Three-Segment Digging*

The unassisted experiment demonstrated that the three-segment soft-robot could locomote in dry GS (Fig. 7). We observed that the soft system was able to move for some time below the surface of the dry granular material; however, we witnessed the presence of a lift force. If the system was not submerged below a depth of five cm, it would rise to the surface after approximately 12-15 minutes of the experiment. A similar lift force has been reported for the simple case of a cylinder traveling through dry granular media [7]. We also observed that the pneumatic lines increased the drag force on the robot as a result of their perpendicular position with respect to the plane of motion.

For these experiments we decided to submerge the system beyond the depth of five cm to approximately eight cm and due

This article has been accepted for publication in a future issue of this journal, but has not been fully edited. Content may change prior to final publication. Citation information: DOI 10.1109/LRA.2019.2911844, IEEE Robotics and Automation Letters



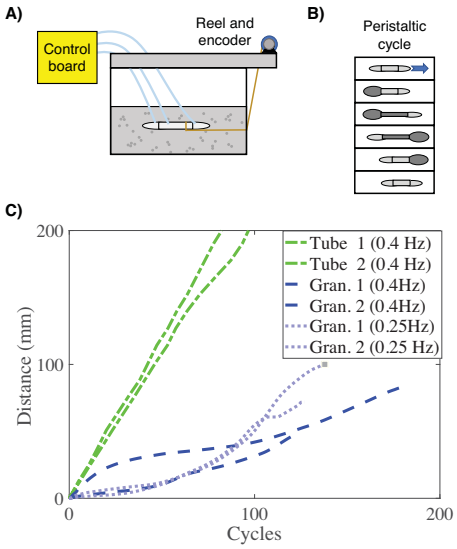


Fig. 7. Tethered experiment setup and data. (A) Diagram of the dry granular experiment using the three-segment tethered soft-robot. (B) Diagram of the three-segment peristaltic cycle used for the unassisted experiments. (C) Graph of the unassisted experiments both in the dry granular environment and the structured tube environment without granular media for comparison.

to this change, resulting in a longer duration of locomotion. The unassisted dry granular experiment with a frequency of 0.4 Hz resulted in an average velocity of 0.10 mm/s and maximum distance traveled of 84 mm (Fig. 7C). The dry granular experiments with PWM switching to achieve a frequency of 0.25 Hz resulted in an average velocity of 0.16 mm/s and a maximum distance traveled of 100 mm. For the case of the structured tube experiment, the average velocity of locomotion was 0.54 mm/s over 200 mm distance of pipe (Fig. 7C).

## IV. Discussion

When we compared the velocity measurements of the constant force experiments for the robot segments with no actuation, the rigid intruder was able to travel a much longer distance for all cases of a constant force being applied. The poor performance of the unactuated soft intruder was likely due to the soft intruders compliance causing it to deform perpendicular to the direction of movement. This deformation likely resulted in an increase in the surface area along the drag direction and thus caused it to experience more drag.

For the comparison of radial expansion and bi-directional bending, we can see that radial expansion outperformed bi-directional bending (Fig. 5). This result from the constant force experiments is likely due to the radial expansion being able to create larger cavitation and disrupt more resistive force chains in the GS. We also observed an acceleration at the beginning of the trials, likely due to an initial loosening of the surrounding particles just before data collection was initiated. Despite this observation, the robot segments almost all reached a steady state after approximately 100 mm of travel (except for the unactuated configurations). The two peaks observed in the data are likely the result of variation in acceleration between experiments.

Similar to the constant force experiments, the unactuated soft intruder experienced the most drag at all velocities for the constant velocity experiments (Fig. 6). Periodic radial expansion experienced the least amount of drag force for all the constant velocities tested. Radial expansion likely experienced the least drag because it moved a large volume of particles, disrupting the most force chains in the granular material. We also observed that bi-directional bending experienced more drag force than the rigid intruder. This result was likely due to material filling the cavitation faster than the intruder moved forward, causing the bi-directional bending to experience more drag force. As expected, the aluminum drag arm did have some contribution to the drag force experienced, however it was consistent for all cases and below the measurement obtained for all the intruder configurations.

In comparing the performance of the tethered robot in granular material to the acrylic tube (ideal case) we noticed that the movement through the granular material resulted in a maximum speed of 18% that of the speed of the ideal case. When comparing the velocity between the two dry granular experiments with different gait frequencies there was a 60% increase in speed for the case where the PWM was adjusted to increase extension in the middle segment. The gait sequence was not optimized for performance, and leaves room for improvement. The result of the unassisted dry granular experiments highlights both the ability of the soft robot to dig despite the anchoring effect of the pneumatic lines, and the challenges of locomoting in dry granular substrates. We did not test the limits of depth at which the system would be capable of locomoting below the surface nor did we examine the anchoring effect due to the pneumatic lines and it is still unknown how much these factors influence the soft robots ability to move.

## V. Conclusion

This paper studies how actuation strategies of a soft robot can reduce drag force during locomotion within dry granular environments. The actuation strategies in this study are inspired by the soft-bristle worm (polychaeta). The results of our work demonstrate that a tethered soft robotic system is capable of locomotion in GS despite (and indeed enabled by) a lack of rigid components. We also show that behaviors observed in the bristle worm can help reduce drag forces associated with locomotion in GS. This study gives insight that could potentially help in the design of future digging robots for applications such as construction, pipe inspection, exploration of hazardous environments, and subsurface exploration on other planets. Future work could investigate untethering the soft robotic system with development of smaller pneumatic components, movement in different mediums such as sand, the effects of penetration angle, depth, the addition of sensors for feedback, gait frequency optimization, and the effect of the orientation of the pneumatic lines on system mobility. Overall the results presented here form the basis for describing the principles of soft robotic interaction in dry granular substrates.

## ACKNOWLEDGMENT

This work was in part supported by the National Science Foundation (NSF) under grant number 1837662. We would also like to show our gratitude to the members of both the Tolley and Gravish Labs for support throughout this project.

## REFERENCES

[1] *Vertical drag force acting on intruders of different shapes in granular media*, ser. European Physical Journal Web of Conferences, vol. 140, Jun. 2017.

[2] N. Gravish, P. B. Umbanhowar, and D. I. Goldman, "Force and flow transition in plowed granular media," *Phys. Rev. Lett.*, vol. 105, no. 12, p. 128301, Sep. 2010.

[3] G. Hill, S. Yeung, and S. A. Koehler, "Scaling vertical drag forces in granular media," *EPL*, vol. 72, no. 1, p. 137, Aug. 2005.

[4] N. A. Frigerio and M. J. Shaw, "A simple method for determination of glutaraldehyde," *J. Histochem. Cytochem.*, vol. 17, no. 3, pp. 176–181, Mar. 1969.

[5] N. Gravish, P. B. Umbanhowar, and D. I. Goldman, "Force and flow at the onset of drag in plowed granular media," *Phys. Rev. E Stat. Nonlin. Soft Matter Phys.*, vol. 89, no. 4, p. 042202, Apr. 2014.

[6] F. Guillard, Y. Forterre, and O. Pouliquen, "Origin of a depth-independent drag force induced by stirring in granular media," *Phys. Rev. E Stat. Nonlin. Soft Matter Phys.*, vol. 91, no. 2, p. 022201, Feb. 2015.

[7] Y. Ding, N. Gravish, and D. I. Goldman, "Drag induced lift in granular media," *Phys. Rev. Lett.*, vol. 106, no. 2, p. 028001, Jan. 2011.

[8] C. Liu, H. Wan, L. Wang, and P. Wu, "Forces on a cylinder intruder associating rotation and plugging/pulling," *Powder Technol.*, vol. 322, pp. 41–46, Dec. 2017.

[9] C. R. Wassgren, J. A. Cordova, R. Zenit, and A. Karion, "Dilute granular flow around an immersed cylinder," *Phys. Fluids*, vol. 15, no. 11, pp. 3318–3330, Nov. 2003.

[10] R. Albert, M. A. Pfeifer, A.-L. Barabási, and P. Schiffer, "Slow drag in a granular medium," *Phys. Rev. Lett.*, vol. 82, no. 1, pp. 205–208, Jan. 1999.

[11] W. Kang, Y. Feng, C. Liu, and R. Blumenfeld, "Archimedes' law explains penetration of solids into granular media," *Nat. Commun.*, vol. 9, no. 1, p. 1101, Mar. 2018.

[12] N. D. Naclerio, C. M. Hubicki, Y. O. Aydin, D. I. Goldman, and E. W. Hawkes, "Soft robotic burrowing device with Tip-Extension and granular fluidization," in *2018 IEEE/RSJ International Conference on Intelligent Robots and Systems (IROS)*, Oct. 2018, pp. 5918–5923.

[13] N. Algarra, P. G. Karagiannopoulos, A. Lazarus, D. Vandembroucq, and E. Kolb, "Bending transition in the penetration of a flexible intruder in a two-dimensional dense granular medium," *Phys Rev E*, vol. 97, no. 2-1, p. 022901, Feb. 2018.

[14] M. S. Verma, A. Ainla, D. Yang, D. Harburg, and G. M. Whitesides, "A soft Tube-Climbing robot," *Soft Robot*, vol. 5, no. 2, pp. 133–137, Apr. 2018.

[15] A. D. Marchese, C. D. Onal, and D. Rus, "Autonomous soft robotic fish capable of escape maneuvers using fluidic elastomer actuators," *Soft Robotics*, vol. 1, no. 1, pp. 75–87, 2014.

[16] C. Christianson, N. Goldberg, S. Cai, and M. T. Tolley, "Fluid electrodes for submersible robotics based on dielectric elastomer actuators," in *Electroactive Polymer Actuators and Devices (EAPAD) 2017*, vol. 10163. International Society for Optics and Photonics, Apr. 2017, p. 101631O.

[17] K. Karakasiliotis, R. Thandiackal, K. Melo, T. Horvat, N. K. Mahabadi, S. Tsitkov, J. M. Cabelguen, and A. J. Ijspeert, "From cineradiography to biorobots: an approach for designing robots to emulate and study animal locomotion," *J. R. Soc. Interface*, vol. 13, no. 119, Jun. 2016.

[18] B. Zhong, Y. O. Aydin, C. Gong, G. Sartoretti, Y. Wu, J. Rieser, H. Xing, J. Rankin, K. Michel, A. Nicieza, and Others, "Coordination of back bending and leg movements for quadrupedal locomotion," in *Robotics: Science and Systems*. crablab.gatech.edu, 2018.

[19] H. Marvi, C. Gong, N. Gravish, H. Astley, M. Travers, R. L. Hatton, J. R. Mendelson, 3rd, H. Choset, D. L. Hu, and D. I. Goldman, "Sidewinding with minimal slip: snake and robot ascent of sandy slopes," *Science*, vol. 346, no. 6206, pp. 224–229, Oct. 2014.

[20] A. G. Winter, V, R. L. H. Deits, D. S. Dorsch, A. H. Slocum, and A. E. Hosoi, "Razor clam to RoboClam: burrowing drag reduction mechanisms and their robotic adaptation," *Bioinspir. Biomim.*, vol. 9, no. 3, p. 036009, Sep. 2014.

[21] R. D. Maladen, Y. Ding, P. B. Umbanhowar, and D. I. Goldman, "Undulatory swimming in sand: experimental and simulation studies of a robotic sandfish," *Int. J. Rob. Res.*, vol. 30, no. 7, pp. 793–805, Jun. 2011.

[22] F. Qian, T. Zhang, W. Korff, P. B. Umbanhowar, R. J. Full, and D. I. Goldman, "Principles of appendage design in robots and animals determining terradynamic performance on flowable ground," *Bioinspir. Biomim.*, vol. 10, no. 5, p. 056014, Oct. 2015.

[23] A. E. Hosoi and D. I. Goldman, "Beneath our feet: Strategies for locomotion in granular media," *Annu. Rev. Fluid Mech.*, Jan. 2015.

[24] C. Laschi, M. Cianchetti, B. Mazzolai, L. Margheri, M. Follador, and P. Dario, "Soft robot arm inspired by the octopus," *Adv. Robot.*, vol. 26, no. 7, pp. 709–727, 2012.

[25] D. Rus and M. T. Tolley, "Design, fabrication and control of soft robots," *Nature*, vol. 521, no. 7553, p. 467, 2015.

[26] T. Umedachi and B. A. Trimmer, "Autonomous decentralized control for soft-bodied caterpillar-like modular robot exploiting large and continuum deformation," in *2016 IEEE/RSJ International Conference on Intelligent Robots and Systems (IROS)*, Oct. 2016, pp. 292–297.

[27] K. M. Dorgan, "Kinematics of burrowing by peristalsis in granular sands," *J. Exp. Biol.*, vol. 221, no. Pt 10, May 2018.

[28] J. Che and K. M. Dorgan, "Mechanics and kinematics of backward burrowing by the polychaete cirriformia moorei," *J. Exp. Biol.*, vol. 213, no. Pt 24, pp. 4272–4277, Dec. 2010.

[29] E. A. K. Murphy and K. M. Dorgan, "Burrow extension with a proboscis: mechanics of burrowing by the glycerid hemipodus simplex," *J. Exp. Biol.*, vol. 214, no. Pt 6, pp. 1017–1027, Mar. 2011.

[30] P. Esselink and L. Zwarts, "Seasonal trend in burrow depth and tidal variation in feeding activity of nereis diversicolor," *Mar. Ecol. Prog. Ser.*, vol. 56, no. 3, pp. 243–254, 1989.

[31] A. A. Calderón, J. C. Ugalde, J. C. Zagal, and N. O. Pérez-Arancibia, "Design, fabrication and control of a multi-material-multi-actuator soft robot inspired by burrowing worms," in *2016 IEEE International Conference on Robotics and Biomimetics (ROBIO)*, Dec. 2016, pp. 31–38.

[32] Y. O. Aydin, J. L. Molnar, D. I. Goldman, and F. L. Hammond, "Design of a soft robophysical earthworm model," in *2018 IEEE International Conference on Soft Robotics (RoboSoft)*, Apr. 2018, pp. 83–87.

[33] S. Seok, C. D. Onal, K.-J. Cho, R. J. Wood, D. Rus, and S. Kim, "Meshworm: a peristaltic soft robot with antagonistic nickel titanium coil actuators," *IEEE/ASME Trans. Mechatron.*, vol. 18, no. 5, pp. 1485–1497, 2013.

[34] B. Kim, M. G. Lee, Y. P. Lee, Y. Kim, and G. Lee, "An earthworm-like micro robot using shape memory alloy actuator," *Sens. Actuators A Phys.*, vol. 125, no. 2, pp. 429–437, Jan. 2006.

[35] L. Xu, H.-Q. Chen, J. Zou, W.-T. Dong, G.-Y. Gu, L.-M. Zhu, and X.-Y. Zhu, "Bio-inspired annelid robot: a dielectric elastomer actuated soft robot," *Bioinspir. Biomim.*, vol. 12, no. 2, p. 025003, Jan. 2017.

[36] T. Nakamura and T. Iwanaga, "Locomotion strategy for a peristaltic crawling robot in a 2-dimensional space," in *2008 IEEE International Conference on Robotics and Automation*, May 2008, pp. 238–243.

[37] K. C. Galloway, P. Polygerinos, C. J. Walsh, and R. J. Wood, "Mechanically programmable bend radius for fiber-reinforced soft actuators," in *2013 16th International Conference on Advanced Robotics (ICAR)*, Nov. 2013, pp. 1–6.

[38] B. Mosadegh, P. Polygerinos, C. Keplinger, S. Wennstedt, R. F. Shepherd, U. Gupta, J. Shim, K. Bertoldi, C. J. Walsh, and G. M. Whitesides, "Pneumatic networks for soft robotics that actuate rapidly," *Adv. Funct. Mater.*, vol. 24, no. 15, pp. 2163–2170, Apr. 2014.

[39] D. P. Holland, E. J. Park, P. Polygerinos, G. J. Bennett, and C. J. Walsh, "The soft robotics toolkit: Shared resources for research and design," *Soft Robotics*, vol. 1, no. 3, pp. 224–230, Sep. 2014.

[40] K. J. Quillin, "Kinematic scaling of locomotion by hydrostatic animals: ontogeny of peristaltic crawling by the earthworm lumbricus terrestris," *J. Exp. Biol.*, vol. 202 (Pt 6), pp. 661–674, Mar. 1999.

[41] A. Pantet, S. Robert, S. Jarny, and S. Kervella, "Effect of coarse particle volume fraction on the yield stress of muddy sediments from marennes oléron bay," *Advances in Materials Science and Engineering*, vol. 2010, Sep. 2010.

[42] N. Gravish and D. I. Goldman, "Effect of volume fraction on granular avalanche dynamics," *Phys. Rev. E Stat. Nonlin. Soft Matter Phys.*, vol. 90, no. 3-1, p. 032202, Sep. 2014.